International Conference on Space Optics—ICSO 2018

Chania, Greece

9–12 October 2018

Edited by Zoran Sodnik, Nikos Karafolas, and Bruno Cugny

Conceptual approaches to the study of efficient bandpass filter design for ultraviolet spaceborne instruments

U. Brauneck

A. Hull

R. Woodruff

J. Sanchez

et al.

International Conference on Space Optics — ICSO 2018, edited by Zoran Sodnik, Nikos Karafolas, Bruno Cugny, Proc. of SPIE Vol. 11180, 111804K · © 2018 ESA and CNES · CCC code: 0277-786X/18/$18 · doi: 10.1117/12.2536083

Conceptual approaches to the study of efficient bandpass filter design for ultraviolet spaceborn instruments

U. Brauneck*[a], A. Hull[b,c], R. Woodruff[d], J. Sanchez [a], D. Apitz [a], T. Westerhoff [e]

[a]Schott Suisse SA, Yverdon-les-Bains, Switzerland, [b]Kendrick Aerospace Consulting LLC, Lafayette, CO, USA, [c]University of New Mexico, Albuquerque, NM, USA, [d]Woodruff Consulting, Boulder, CO, USA, [e] Schott AG, Mainz, Germany

ABSTRACT

In support of a spaceborne astrophysics instrument design, we have studied high UV filter efficiency and strong transmission blocking out to the end of Si response at 1100nm. For filters at wavelengths 297.5nm/338.5nm/379.5nm, these attributes are achieved with the combination of hard sputtered dielectric coatings on colored glass substrates. The filterglass substrates can be used to suppress ghost images caused by reflection at the exit face which is a common problem of all interference filter designs. Known disadvantages of filterglasses like solarization or autofluorescence are discussed and possible ways to mitigate are discussed. At two shorter wavelengths, 215.5nm and 256.5nm, metal-dielectric Fabry-Perot stacks are applied on fused silica. Those traditional designs are advantageous due to their efficient blocking up to the mid IR range and economic low number of layers. We discuss the different design possibilities of metal-dielectric filters and ways to improve the steepness of the slopes. Resulting spectra are expressed.

Keywords: optical filter, bandpass filters, interference filters, filter assembly, spaceborn instrumentation, astronomy

1. INTRODUCTION

Bandpass filters in the ultraviolet spectral region recently gain more importance in spaceborn instruments to study fundamental questions about galaxy evolution by carrying out UV imaging and spectroscopic surveys of galaxies and combining the findings with data obtained by other survey telescopes. Concepts for Probe-class mission like CETUS (Cosmic Evolution Through Ultraviolet Spectroscopy) make use of the described bandpass designs. The CETUS mission and its system engineering was already described in previous publications [1,2,3]. The optical design was described in [4,5] and detailed explanations of the telescope were given in [6]. The camera and spectroscopic instruments were presented in [7,8,9]. The UV-bandpass activities of SCHOTT were already developed many decades ago [10] and have been expanded in the interference coating competence center of SCHOTT Suisse S.A. in Switzerland.

*ulf.brauneck@schott.com; phone +41 24 423 5918; www.schott.com

2. COATING DESIGN APPROACHES FOR BANDPASSES IN THE ULTRAVIOLET

The present study takes the idea of filter sets employed by the Sloan Digital Sky Survey (SDSS) which has become a standard in imaging surveys in optical astronomy and applies it to the near ultraviolet spectral region. The Filters have to be contiguous in wavelength, so all spectral features of emissions of astronomical objects can be detected. With a set of the described filter designs, a camera could cover the range between 200 and 400nm and thus observe galaxies already observed by Subaru's Hyper-Suprime Cam covering 400 – 1300 nanometers.

Due to the continguousness of the filters, the central wavelengths and full widths at half maximum were adequately chosen. A maximum transmission should be achieved in the filter passbands and they should provide a maximum blocking outside the bandpass from about 200nm to the NIR. Much importance was given to the minimization of the backside reflection of the filters, so the substrates were chosen to have absorption outside the passbands to attenuate the high reflectance of the filter coatings that could cause ghost images due to multiple reflections. For that reason SCHOTT filterglasses present a solution for the bandpass wavelengths 297.5nm, 338.5nm and 379.5nm where appropriate glasses exist. In the UV-A and UV-B wavelengths the filterglass types where chosen from the N-WG, UG and BG-groups. While N-WG glasses provide a longpass characteristic to absorb in the UV, the UG and BG-types have bandpass-characteristics that absorb parts of the UV and the red and NIR range. Due to the tendency of UG/BG-glasses to solarize

in strong UV-irradiation this property should be taken into account for a specific application. The disadvantage, that some filterglasses show a problematic climatic resistance can be mitigated by a coating with dense metal oxide coatings. The sharp cut-on and cut-off to form a steep bandpass cannot be achieved only by filterglass components so interference layer systems are indispensable. To gain good transmission in the UV-A and UV-B region and good durability of the coatings, we chose HfO_2 and SiO_2 multilayer stacks to be deposited by magnetron sputtering.

For the bandpass wavelengths 215.5nm and 256.5nm in the UV-C region it is not possible to use absorptive filterglass as they would cut into the passband of the filters. For those wavelengths fused silica substrates were selected. Metal-dielectric Fabry-Perot filter coatings represent the most efficient way to achieve a bandpass characteristic in the UV-C with deep blocking until the far infrared. This type of coatings are humidity sensitive and have to be hermetically mounted with a coverglass in a filtermount allowing for an airspace between the two substrates. The alternative designs with all-dielectric layer systems would require hundreds of layers to achieve a blocking up to 1050nm and higher order interferences would present a high risk of reflection peaks in the passband regions. Therefore that alternative was not persued.

The complete set of filter designs are proposed to consist of 2 substrates assembled in a filter mount with an airspace between them. This would be either 2 fused silica substrates for the UV-C filters or 2 filterglass components for the UV-A and UV-B filters. A good transmitted wavefront of about lambda/4 over a clear aperture of e.g. 70mm can be guaranteed by maintaining a parallelity of several arcseconds even when the substrates are bowed by internal stress of the filter coatings.

2.1. Bandpass designs for the UV-A and UV-B region

The bandpass 379.5-41 contains N-WG280 at the light incidence side with a thickness of 3 mm and BG25 with a thickness of 2 mm at the detector side. The filter coatings were divided into a bandpass-coating on the entrance side and an red-blocking coating on the internal side. The BG25 on the exit side has a double sided antireflection coating. The principle of composition can be seen in table 1. The calculation of the theoretical performances takes the absorption of substrates and filter layers into account. The calculated transmission spectrum can be seen in Fig. 1 it can be seen that the blocking of the filter is better than 10^{-4} below 350 nm and 10^{-4} average from 410 to 1030 nm. In figure 2 the backside reflection (BR) spectrum is shown for the whole filter stack (black solid curve) and for the case if the filter would not consist of absorbing filterglass. It can be seen, that the suppression of the backside reflection is very efficient.

Substrates	Coatings
	Bandpass coating
N-WG280, 3 mm thickness	
	Red-IR-blocking filter
Airspace 1 mm	
	Antireflection coating
BG25, 2 mm thickness	
	Antireflection coating

Table 1: filter design of bandpass 379.5-41 showing substrate and coating arrangements. Upper side is light entrance side and lower side is detector side.

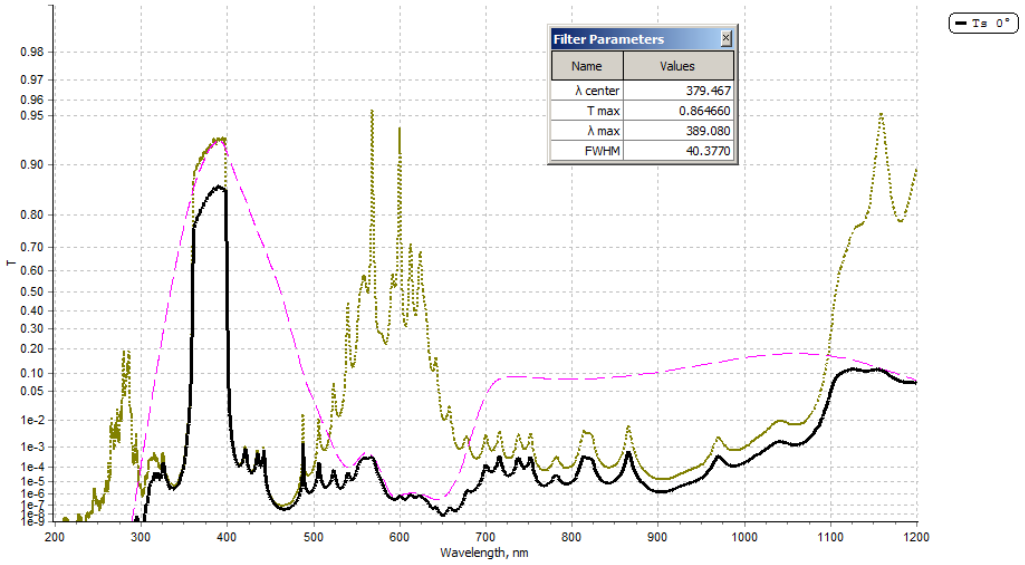

Fig. 1 shows the calculated transmission curve in diabatic scale of the bandpass 379.5-41 (thick solid line), the transmission curve of the filter coatings on N-WG280 (brown dotted curve) and the transmission curve of the antireflection coatings on BG25 (magenta dashed line). The full width at half maximum of the design is 40.38 nm and the transmission maximum is 86.5%.

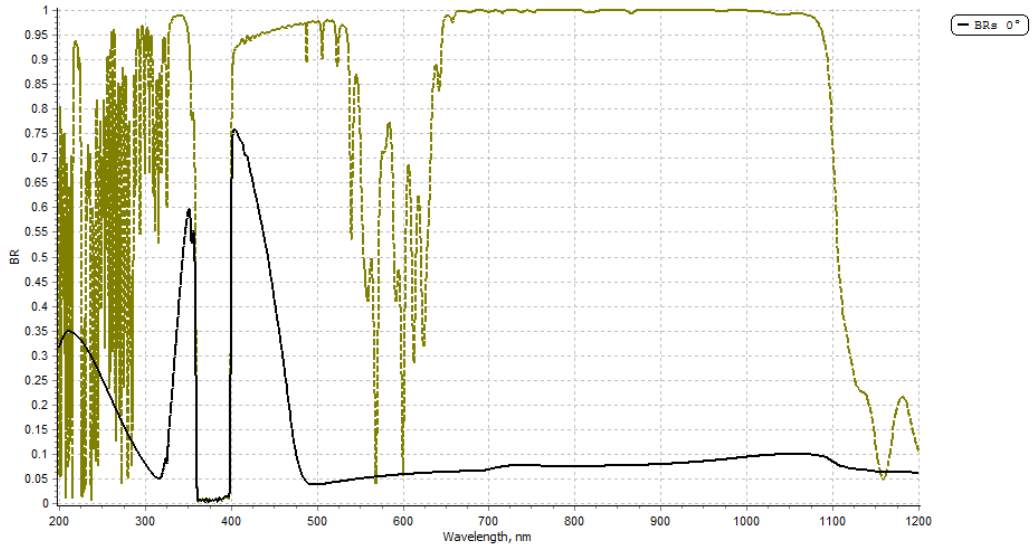

Fig. 2 shows the effect of the suppression of backside reflection by the use of the filterglasses N-WG280 and BG25 in the bandpass 379.5-41. The black solid curve shows the backside reflection of the whole filter stack. The dashed brown curve shows the backside reflection if the filter would consist of only the filter coatings without filterglass substrates.

The design curves are shown for collimated light at an angle of incidence perpendicular to the filter surface. To adapt the designs for a specific numerical aperture it would require only a minor adaptation. The filter centering would shift a bit to the blue side.

The bandpass 338.5-41 is composed of N-WG280 at the light incidence side with a thickness of 3 mm and UG5 with a thickness of 3 mm at the detector side. The filter coatings were arranged very similarly to the BP379.5-41: a bandpass-coating on the entrance side and an red-IR-blocking coating on the internal side. In fact the order of coatings does not play a major role due to the bandpass characteristics of the filterglass on the detector side. The UG5 on the exit side has a double sided antireflection coating to protect the humidity sensitive glass and of course to minimize reflections an maximize transmission. The calculated transmission spectrum can be seen in figure 3. The black solid curve in figure 3 represents the whole filter stack, the brown dotted curve is the transmission of the filter coatings on N-WG280 (first component) and the magenta dashed curve represents the transmission of the UG5 with antireflection coatings (second component). The full width at half maximum is 41nm and maximum transmission 81.9% (see insert of Fig.3). The average blocking of BP338.5-41 is better than 10^{-4} from 200-315 nm and from 360-1070nm. In figure 4 the backside reflection (BR) spectrum is shown for the whole filter stack (black solid curve) and for the hypothetical case if no filterglass substrates would have been used (brown dashed curve).

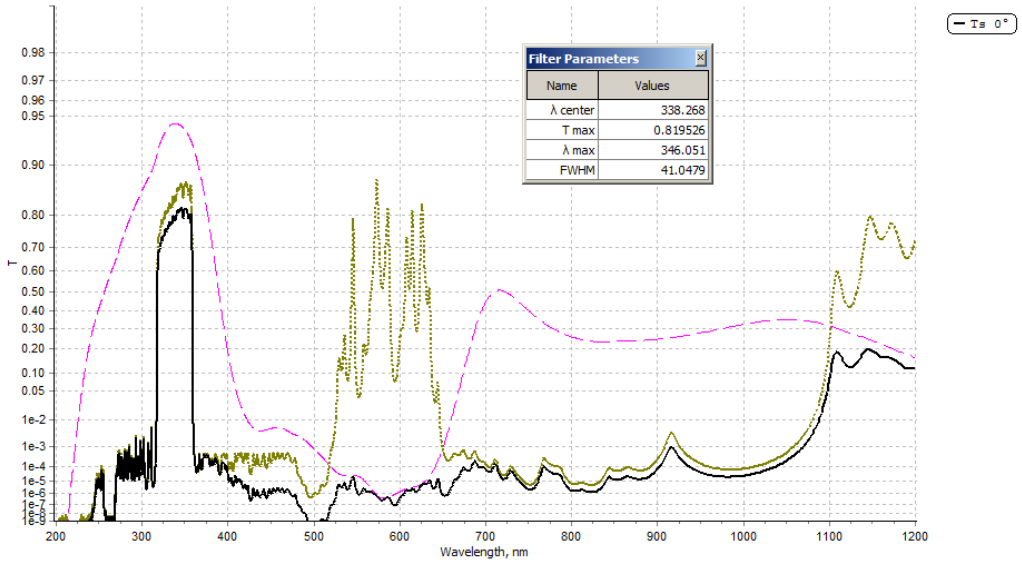

Fig. 3 shows the calculated transmission curve in diabatic scale of the bandpass 338.5-41 (thick solid line), the transmission curve of the filter coatings on N-WG280 (brown dotted curve) and the transmission curve of the antireflection coatings on UG5 (magenta dashed line). The full width at half maximum of the design is 41.0 nm and the transmission maximum is 81.9%.

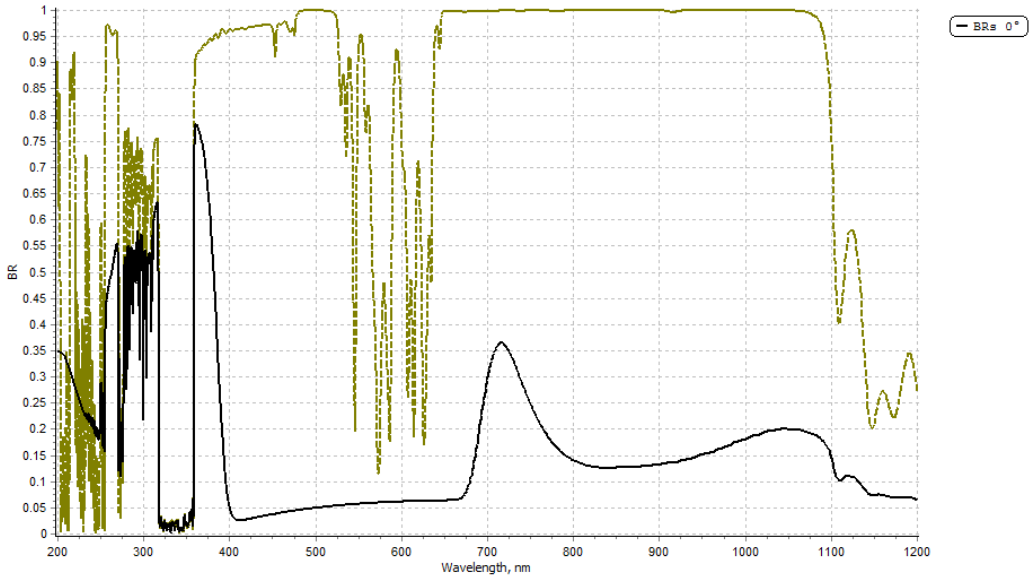

Fig. 4: The solid curve shows the backside reflection taken into account the whole filter stack including filterglasses N-WG280 and UG5. The dashed brown curve represents the hypothetical case, when no filterglasses would be used.

For the filter BP297.5-41 we saw, that from the different filterglasses UG11 represents the best compromise between good transmission at 297.5nm and blocking until 1100nm. However while maintaining a transmission level of more than 80% one needs to compromise on blocking in the near infrared. In addition we saw, that it is very difficult to block the range 850-900nm with interference layers as a higher order interference then falls into the passband range of the filter. For that reason we chose to use fused silica at the light incidence side with a thickness of 2 mm and UG11 with a thickness of only 1 mm at the detector side. On the entrance side of the fused silica we chose to design a bandpass coating that also blocks the residual transmission peak of UG11 around 720nm and the region between 900 and 1100nm. On the exit face we chose to design an antireflection layer. The UG11 on the exit side has a double sided antireflection coating to protect the humidity sensitive filterglass and to minimize reflection. The calculated transmission spectrum can be seen in figure 5. The black solid curve in figure 5 represents the whole filter stack, the brown dotted curve is the transmission of the filter coating and antireflection coating on fused silica (first component) and the magenta dashed curve represents the transmission of the UG11 with antireflection coatings (second component). The full width at half maximum is 41.9 nm and maximum transmission 83.8% (see insert of Fig.5). The average blocking of BP297.5-41 is 10^{-4} from 200-270 nm and $3x10^{-4}$ from 325-1100nm. In figure 6 the backside reflection (BR) spectrum is shown for the whole filter stack (black solid curve) and for the hypothetical case if no filterglass substrates would have been used (brown dashed curve).

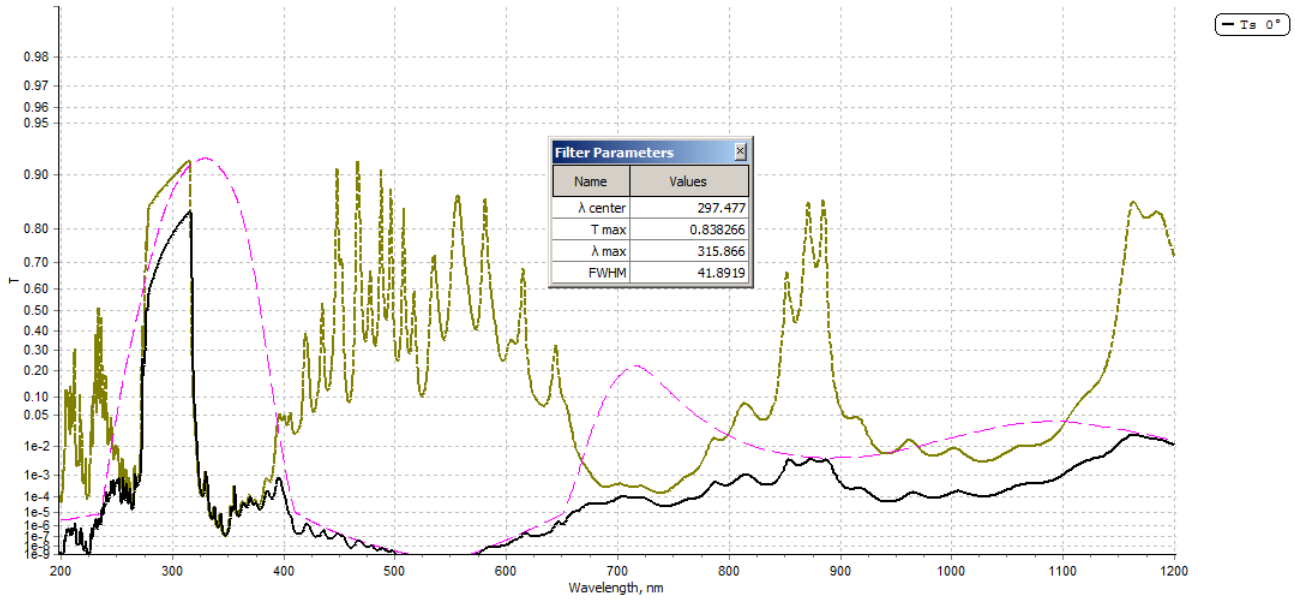

Fig 5 shows the transmission spectrum of BP297.5-41 (all components: black solid curve) as well as the curve of the first component fused silica with bandpass coating on entrance side and antireflection coating on exit face (brown dotted curve) and the curve of the second component UG11 with double-sided antireflection coating (magenta dashed curve).

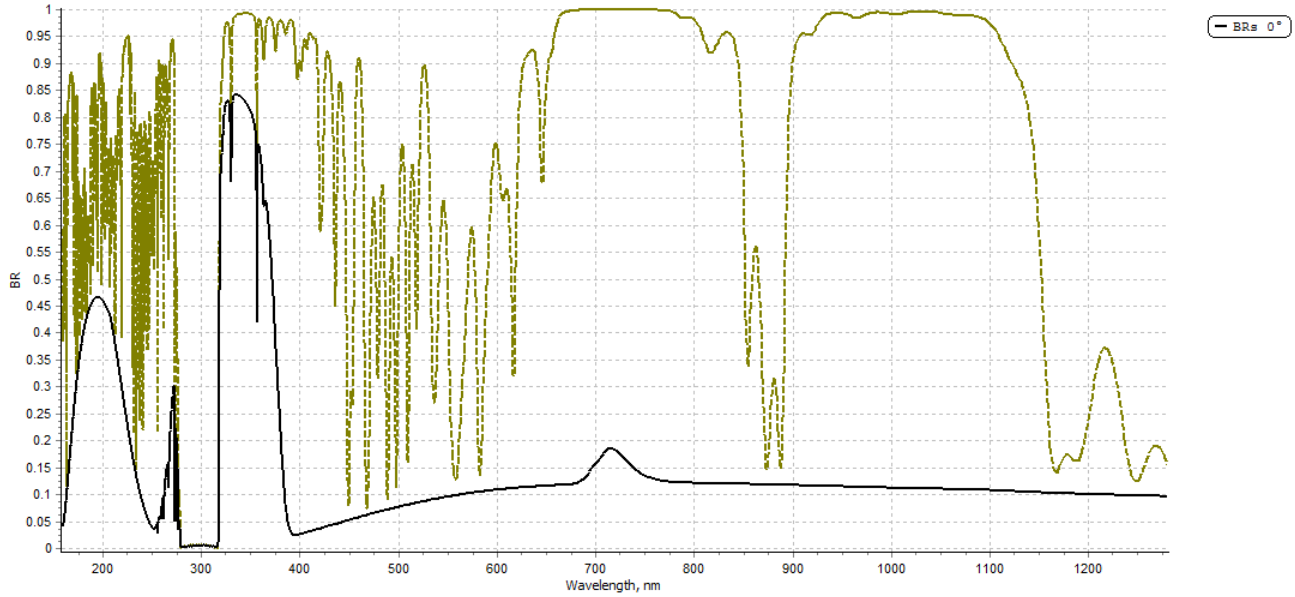

Fig. 6: The solid curve shows the backside reflection of the whole filter arrangement for BP297.5-41 including fused silica with filtercoatings and the filterglass UG11 with antireflection coatings. The dashed brown curve represents the hypothetical case, when no filterglasses would be used and no backreflectance would be absorbed.

The coatings of the three filters in the UV-A and B range was proposed to be produced with plasma assisted reactive magnetron sputtering (PARMS). The PARMS **Błąd! Nie można odnaleźć źródła odwołania.** process results in very dense and humidity resistant coatings with a very low temperature shift. The mechanical and environmental resistance of the coatings are excellent due to the high density of the metal oxide films. The coatings resist of course cleaning with alcohol or acetone.

2.2. Bandpass designs for the UV-C region

For the filters BP215.5-41 and BP256.5-41 we proposed a conventional electron-beam evaporated metal dielectric Fabry-Perot bandpass system of type SCHOTT type KMZ40 [12] consisting of aluminium and cryolithe layers. The KMZ40 transmission characteristic shows a Gaussian shape and cannot achieve the steep spectral slopes of the all-dielectric bandpasses proposed for the filter wavelengths 297.5nm, 338.5nm and 379.5nm. It is however possible to improve the slope of the filters by additional all dielectric filters.

Table 2 shows the arrangement of the components. An antireflection coating of the outside faces and the one remaining inside face would gain only 2-3% transmission due to absorption of the KMZ40 layersystem. For that reason it was not proposed to apply.

Substrates	Coatings
Fused silica, 2 mm thickness	
	Metal-dielectric bandpass (SCHOTT type KMZ 40)
Airspace 1 mm	
Fused silica, 2 mm thickness	uncoated

Table 2: composition of BP215.5-41 and BP256.5-41. The fused silica substrate would be mounted hermetically with an airspace between them in an anodized metal ring.

Due to their composition, the transmission level is considerably lower than the all-dielectric layersystems but the blocking range extends far into the infrared. Figure 7 shows the calculated transmission spectra of both metal-dielectric bandpasses. BP256.5-41 shows a maximum transmission of 40% and the full width at half maximum 40.6 nm, the integrated blocking from 315-1200nm is $3x10^{-6}$. BP215.5-41 has a maximum transmission of 37% and FWHM is 40.7nm, the integrated blocking from 275-1200nm is $2x10^{-6}$. Figure 8 shows the backside reflectance of both UV-C filters. It can be noted that the reflectance could not be suppressed by the use of filterglasses.

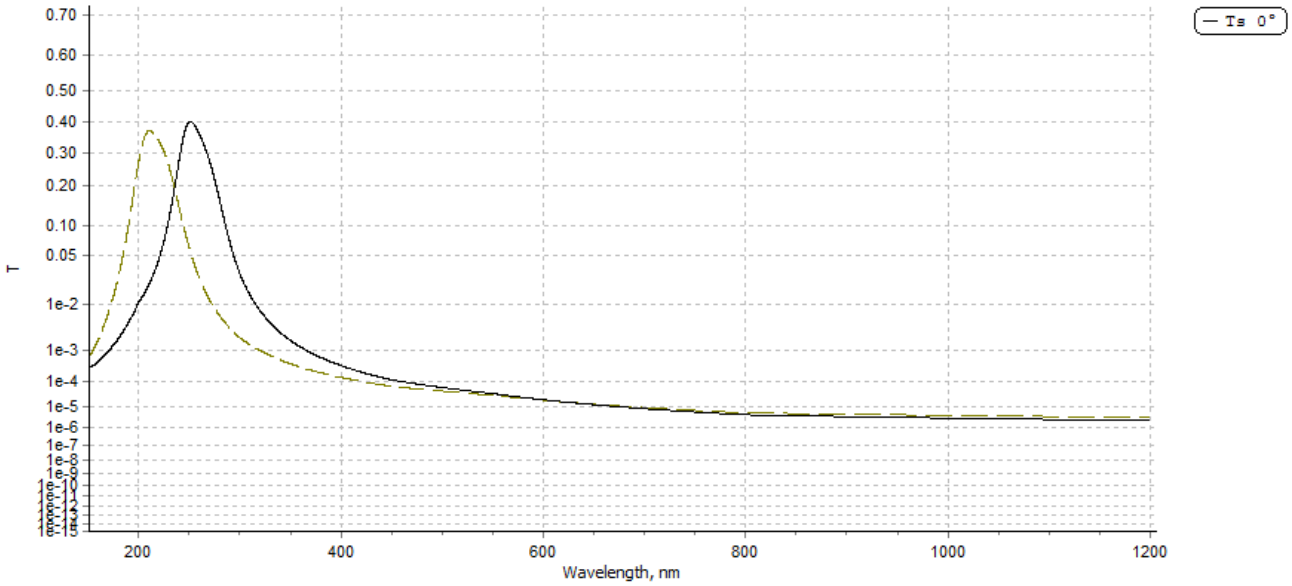

Fig.7: calculated transmission spectrum of the metal-dielectric bandpass system BP256.5-41 (black solid line) and BP215.5-41 (brown dashed line).

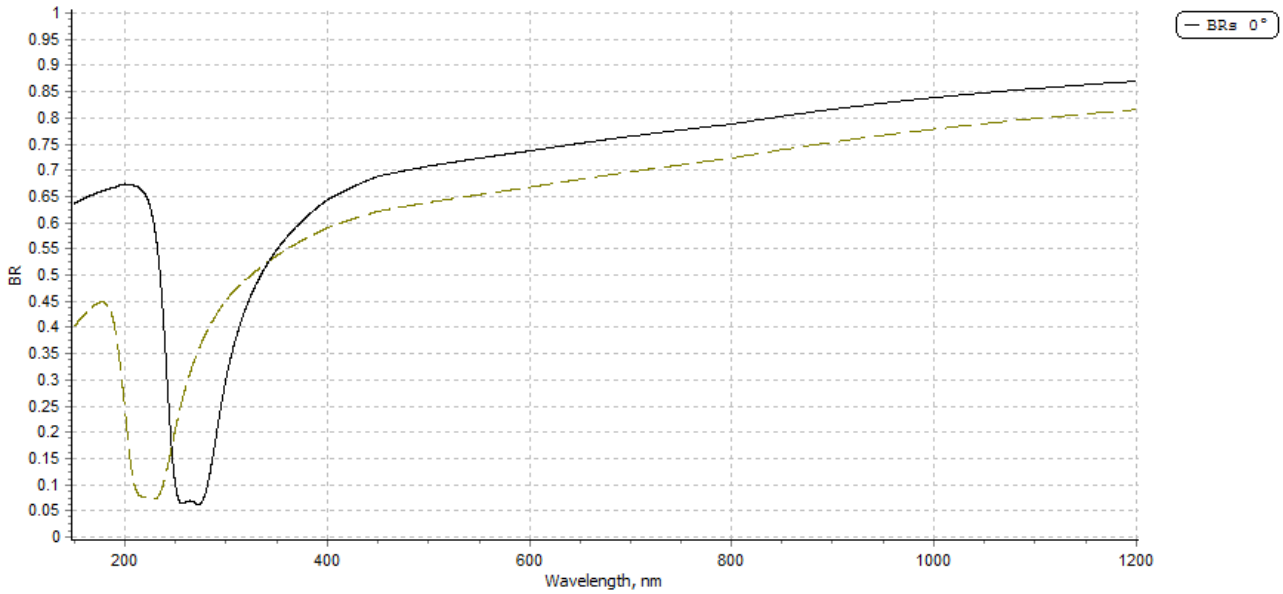

Fig. 8 calculated backside reflection of BP256.5-41 (black solid line) and BP215.5-41 (brown dashed line): The filters are composed of 2 fused silica substrates mounted with an airspace in between and the coating is on one of the internal face to protect the coating from humidity as the coating materials are hydrophilic. As there are no filterglasses available that transmit sufficiently below 250 nm the level of backside reflection is considerably higher than for the proposed UV-A and UV-B filters.

3. SUMMARY

We present a theoretical study for the designs of a set of bandpass filters for the UV-A, UV-B and UV-C range that are contiguous in wavelength to conduct imaging surveys following the idea of Sloan Digital Sky Survey (SDSS). This set of filters would be for example suitable for the CETUS project with required centerwavelengths 215.5 nm / 256.5 nm / 297.5 nm / 338.5 nm and 379.5 nm and FWHM of 41 nm. The blocking should be as good as possible from 200 nm to about 1100 nm. This design study based on all-dielectric hard sputtered coatings on colorglass substrates for the wavelengths 297.5 nm / 338.5 nm / 379.5 nm. It was shown that the use of filterglass substrates can suppress ghost images caused by reflection on the exit face and in addition improve the blocking in the required range. For the wavelengths 215.5 nm and 256.5 nm a conventionally evaporated design of metal-dielectric Fabry-Perot stacks of SCHOTT type KMZ40 was chosen on fused silica substrates.

REFERENCES

[1] Heap, S., Hull, A., et al., “CETUS: An innovative UV probe-class mission concept,” Proc. SPIE 10398, (2017).
[2] Heap, S., Danchi, W., et al., “The NASA probe-class mission concept, CETUS (Cosmic Evolution Through Ultraviolet Spectroscopy), SPIE 10398, (2017).
[3] Purves, L., “Mission systems engineering for the Cosmic Evolution Through UV Spectroscopy (CETUS) space telescope concept,” Proc. SPIE 10401, (2017).
[4] Woodruff, R., et al., “Optical design for CETUS: a wide-field 1.5m aperture UV payload being studies for a NASA probe class mission study,” Proc. SPIE 10401, (2017).
[5] Woodruff, R., Danchi, W., et al., “Optical design for CETUS: a wide-field 1.5m aperture UV payload being studies for a NASA probe class mission study,” AAS 140.15, (January 9, 2018).
[6] Hull, A., Heap, S., et al., “The CETUS probe mission concept 1.5m optical telescope assembly: A high A-Omega approach for ultraviolet astrophysics, Proc. SPIE 10699, (2018).

[7] Kendrick, S., Woodruff, R., et al., "Multiplexing in Astrophysics with a UV multi-object spectrometer on CETUS, a Probe-class mission study," Proc. SPIE 10401, (2017).
[8] Kendrick, S, Woodruff, R., et al., "UV spectroscopy with the CETUS Ultraviolet multi-object spectrometer (MOS)," AAS 140.08, (January 9, 2018).
[9] Kendrick, S, Woodruff, R., et al., "UV capabilities of the CETUS multi-object spectrometer and NUV/FUV camera," Proc. SPIE 10699, (2018).
[10] Hull, A., Reichel, S., Brauneck, U., Naulin, V., Marin-Franch, A., "The legacy of filter design and how that has extended into current choices for advanced astronomical filter", Proc. SPIE 9912-101, Edinburgh 2016
[11] Scherer, M. et al., "Innovative production of high quality optical coatings for applications in optics and optoelectronics," 47th annual technical conference proc. of the society of vacuum coaters, 179, (2004).
[12] SCHOTT interference Filters & Special filters catalog, Properties 2015, https://www.schott.com/d/advanced_optics/51b6d5ad-b48b-440f-9349-95d28d7d611a/1.2/schott-interference-filters-and-special-filters-properties-2015-eng.pdf last accessed 8th August 2018.